

On the significant impact of the moderate geomagnetic disturbance of March 2008 on the equatorial ionization anomaly region over Indian longitudes

N. Mridula,¹ G. Manju,¹ Tarun Kumar Pant,¹ Sudha Ravindran,¹ Lijo Jose,¹ and Shobana Alex²

Received 3 March 2011; revised 19 April 2011; accepted 21 April 2011; published 29 July 2011.

[1] The response of the equatorial and low-latitude ionosphere plasmasphere system to the moderate geomagnetic disturbance of March 2008 is the subject of this paper. This study for the first time reports large plasmaspheric electron content modulation at equatorial and low-latitude regions over India during a moderate geomagnetic disturbance. This paper also presents, for the first time, five station tomograms encompassing the entire EIA region and unequivocally demonstrates the effectiveness of tomographic technique in investigating storm-induced modulations of the equatorial ionization anomaly. The present study has been carried out using the total electron content values derived from GPS and Coherent Radio Beacon Experiment (CRABEX) data over Indian longitudes, ionosonde data at Trivandrum (8.5°N, 77°E) and Delhi (28°N, 78°E), and the geomagnetic field data from Trivandrum and Alibag.

Citation: Mridula, N., G. Manju, T. K. Pant, S. Ravindran, L. Jose, and S. Alex (2011), On the significant impact of the moderate geomagnetic disturbance of March 2008 on the equatorial ionization anomaly region over Indian longitudes, *J. Geophys. Res.*, 116, A07312, doi:10.1029/2011JA016615.

1. Introduction

[2] Quiet time equatorial ionosphere is controlled mainly by electrodynamical forcing which causes the generation of a large number of processes like the equatorial electrojet (EEJ), the counter electrojet (CEJ), the equatorial ionization anomaly (EIA), and the nighttime phenomenon of equatorial spread F (ESF). EEJ is an intense band of eastward current system that flows, during daytime, along the dip equator at an altitude centered at around 105 km. EIA is characterized by a double humped latitudinal distribution of electron density, with a trough at the magnetic equator and a crest at $\pm 15^\circ$ to 20° dip latitude on either side of the magnetic equator [Appleton, 1946]. The EIA starts to form at around 09:00 LT (Indian Standard Time) with the crests close to the dip equator and gains in strength and moves poleward in the afternoon period. During evening hours, close to sunset, the EIA begins to recede. Significant storm-induced changes in the quiet time patterns of EIA have been reported earlier by many researchers [Sreeja *et al.*, 2009, and references therein].

[3] Response of the polar thermosphere-ionosphere system to the geomagnetic disturbances is direct [Lu *et al.*, 1998]. But the equatorial and low-latitude ionosphere ther-

mosphere system response to the storm is mainly due to the indirect effects caused by the electrodynamical and neutral dynamical coupling of low latitude and high latitude [Burrage *et al.*, 1992; Fuller-Rowell *et al.*, 1997; Sastri *et al.*, 2003, and references therein].

[4] The storm time response of the equatorial ionosphere is mainly controlled by the electric field disturbances of magnetospheric origin [Fejer and Emmert, 2003]. The equatorial zonal electric field gets modified during geomagnetic disturbances mainly by the prompt penetration electric field and the disturbance dynamo electric field [Blanc and Richmond, 1980; Fejer and Scherliess, 1997]. These fields are caused by magnetosphere-ionosphere interaction, leading to a redistribution of the ionospheric plasma, and hence cause tremendous changes in total electron content (TEC-integrated free-electron density along the signal path [Tsurutani *et al.*, 2004, and references therein]). In addition to the large modulations in the TEC distribution over the EIA region, significant changes occurring in the plasmaspheric electron content (PEC) during intense storms have also been reported [Manju *et al.*, 2008].

[5] Although studies related to PEC modulations during intense geomagnetic storms have been carried out earlier, no studies have been done to study the PEC response during moderate geomagnetic disturbances. In the present paper, the impact of a moderate geomagnetic disturbance on the ionosphere of EIA region and also the plasmaspheric electron content is discussed for the first time. The response of the equatorial and low-latitude ionosphere plasmasphere system to the moderate geomagnetic disturbance of March

¹Space Physics Laboratory, Vikram Sarabhai Space Centre, Trivandrum, India.

²Indian Institute of Geomagnetism, Mumbai, India.

Table 1. Geographic and Geomagnetic Latitude Coordinates and Corresponding Longitudes for All the Stations for Which Ionospheric Data Have Been Used in This Study

Station	Latitude Geographic (°N)	Latitude Geomagnetic (°N)	Longitude Geographic (°E)
Trivandrum	8.5	0.5	77.0
Bangalore	12.98	4.98	77.6
Hyderabad	17.8	9.8	78.0
Bhopal	23.2	15.2	77.2
Delhi	28.67	20.67	77.2
Alibagh	18.6	10.6	72.9

2008 is the subject of this paper. This study for the first time reports large PEC modulation at equatorial and low-latitude regions over India during a moderate geomagnetic disturbance. This paper also presents, for the first time, five station tomograms encompassing the entire northern EIA region and unequivocally demonstrates the effectiveness of tomographic technique in investigating storm-induced modulations of the EIA. The study of the response of ionosphere plasmasphere system during a moderate disturbance is all the more important in the wake of increased satellite and GPS systems for positioning and navigation purposes.

2. Data and Method of Analysis

[6] The present study has been carried out using the TEC values derived from GPS and Coherent Radio Beacon Experiment (CRABEX) data over Indian longitudes, ionosonde data at Trivandrum (8.5°N, 77°E) and Delhi (28°N, 78°E), and the geomagnetic field data from Trivandrum and Alibagh. The absolute slant GPS-TEC values are derived from the carrier phase delays and pseudoranges of the GPS signals at L1 and L2 frequencies. The slant total electron content (STEC) is then converted to absolute vertical TEC (VTEC) following the standard procedure using the mapping function:

$$\text{VTEC} = \text{STEC} \cos(\chi) \quad (1)$$

where χ is the zenith angle at ionospheric pierce point (IPP) which is estimated from the satellite elevation angle. Here, only those raypaths with elevation angles greater than 50° are used. *Rama Rao et al.* [2006] showed that an elevation angle cutoff of >50° is ideally suited to represent the TEC over the Indian sector. IPP is the point where the line joining the satellite and the receiver cuts the ionosphere at an altitude where the entire ionization is assumed to be concentrated (single shell model). The TEC values obtained using the GPS system represent the electron content along the line of sight up to the satellite altitude (~20,000 km), while those obtained from low Earth orbiting satellites segment of CRABEX system (using beacon transmissions at 150 and 400 MHz from low Earth orbiting satellites) represent the electron content up to ~1000 km.

[7] The CRABEX Network (CRABNET) consists of a chain of receivers located in the 77°E–78°E meridian. The stations are located at Trivandrum (8.5°N geographic, 0.5°N geomagnetic), Bangalore (12.98°N geographic, 4.98°N geomagnetic), Hyderabad (17.8°N geographic, 9.8°N geomagnetic), Bhopal (23°N geographic, 15°N geomagnetic),

and Delhi (28.67°N geographic, 20.67°N geomagnetic). Table 1 shows the locations of all these receivers. In the present study, the data from the five stations, namely, Trivandrum, Bangalore, Hyderabad, Bhopal, and Delhi, are used. Figure 1 depicts the satellite raypaths simulated for the pass of 27 March 2008 at 11:15 LT. Only few raypaths are shown for clarity. Figure 1 shows the tomographic reconstruction plane which evidently encompasses the entire Indian northern EIA region from the trough to the crest. For all the passes this plane remains more or less same.

[8] At each station, phase coherent signals of 150 and 400 MHz transmissions from the Navy Ionospheric Monitoring System (NIMS) satellites are received, and the differential Doppler between them is estimated. This differential Doppler is proportional to the line of sight total electron content (TEC). The measured data, which are the relative phase between 150 and 400 MHz, in the present case, are proportional to the relative slant TEC (STEC) along the propagation path of the signal as

$$\phi = C_D \times \text{STEC} \quad (2)$$

where ϕ is measured in radians, STEC is in m^{-2} , and $C_D = 1.6132 \times 10^{-15}$ for NIMS satellites [*Leitinger, 1994*]. As mentioned earlier, the TEC measurements at each station are only the relative TEC estimates, which have an inherent $2n\pi$ ambiguity. The conversion of the relative TEC to absolute TEC needs the estimation of the unknown phase offset. Several approaches are generally used for the estimation of this TEC offset. The simplest among them is the use of the model-generated TEC values. However, this method is highly inaccurate because of the limitations of the models to represent the day-to-day variability of the electron content in any region especially in the equatorial region.

[9] In this context, a method to estimate the unknown phase offset, using the TEC data, is developed by *Leitinger et al.* [1975]. This method requires the relative TEC data from two near-by stations. For two stations, aligned in a fixed longitude monitoring the same satellite pass, it is assumed that the vertical TEC from each receiver is same at specific ionospheric latitude. This RVTEC is observed simultaneously by both the receiving stations. Then chi square fits are applied to get the constants which are added to RSTEC to get absolute STEC. The absolute STEC values

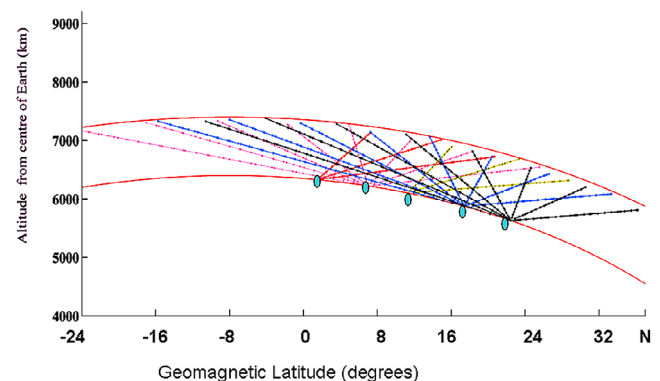


Figure 1. The raypaths of the satellite in the entire region covering the northern EIA from the trough to the crest for pass on 27 March 2008 at 11:15 LT.

are used for tomographic imaging. Nevertheless, the basic requirement for ionospheric tomography is that there must be a chain of receivers aligned along the same longitude (since the satellites are polar orbiting), which gives time-synchronized TEC data with maximum overlapping.

[10] In tomography, these TECs measured simultaneously over a latitudinal chain of receivers are inverted to obtain the latitude-altitude distribution of electron density of the ionosphere. Mathematically, the tomography problem can be stated as

$$Y_i = \sum A_{ij}x_j, \quad (3)$$

where Y_i corresponds to the i th measurement (TEC), x_j is the unknown electron density in the j th pixel, and A_{ij} is the length of the ray element in the pixel defined by i and j . To compute the elements of the matrix A , the geocentric circular grids are constructed in the region. This is more realistic, especially when the region to be imaged covers a large latitude region.

[11] In this case, the ionospheric region is divided into grids in the θ (latitude) and r (altitude) directions. To compute the ray elements A_{ij} , we need to find out the intersections between the ray (straight line) and the concentric circles (r grids). This means that basically we need to calculate the intersections with the straight line and the circle defined as $x^2 + y^2 = (R_E + h)^2$, where R_E is the radius of the Earth and h is the altitude. Similarly, we need to calculate the intersections between the ray (straight line) and the θ lines. After these intersections are computed, it is straightforward to estimate the ray lengths in each grid and to arrange them as the geometry matrix. The position of the satellite at each second is determined by running the track star program. The resolution is 1° (horizontal) \times 50 km (vertical) for all the images, and the altitude extent for tomographic reconstruction is from 100 to 1000 km. Once the TEC values and the geometry matrix are computed, we can reconstruct the tomographic image using the algebraic reconstruction technique (ART) algorithm to solve equation (3). This inversion procedure, which was first introduced by *Austen et al.* [1988] for ionospheric tomography, is being widely used. The iteration starts from an initial guess x^0 . The solution is obtained using the typical step

$$x^{k+1} = x^k + \lambda_k \frac{y_i - \langle a^i, x^k \rangle}{\|a^i\|^2} a^i, \quad (4)$$

where x^k is the solution after k iterations, y_i are the TEC data, a^i are the elements of the matrix A , and λ_k is the relaxation parameter. It was seen that after 5–10 iterations the solution usually converged. An initial guess given was that the International Reference Ionosphere (IRI) model generated electron densities. Further details of tomographic technique are given by *Thampi et al.* [2004, 2007] and *Sreelatha et al.* [2005].

[12] The PEC estimates have been made by taking the differences between the GPS (<20,000 km) TEC and the CRABEX (<1000 km) derived ionospheric TEC (IEC) values estimated nearly simultaneously. PEC percentage is given by the relation

$$\text{PEC percentage} = (\text{PEC}/\text{GPS TEC}) \times 100. \quad (5)$$

ΔH values (the deviation of the horizontal component of the Earth's magnetic field H from its mean nighttime level) were obtained using a ground-based proton precession magnetometer.

3. Results and Discussion

3.1. Interplanetary Conditions During the March 2008 Geomagnetic Disturbance

[13] Figure 2a depicts the temporal variation of Dst for the period of 24–31 March 2008. From 25 March 2008 onward a series of minor disturbances are evident. The moderate storm sudden commencement occurs close to noon on 26 March 2008. The main phase maximum is attained by around midnight of the same day. This is followed by the recovery phase and a series of recurrent disturbances which persist till 31 March 2008. From the temporal evolution of IMF B_z (Figure 2b), it is seen that close to noon time on 26 March 2008, there is evidence of southward turning of IMF B_z , with the largest magnitude of southward turning being -10 nT. Figure 2b shows the solar wind speed for the period of 24 March 2008 to 31 March 2008. Solar wind shows an increase in the morning sector of 26 March 2008 and remains high (almost 700 km/s) up to 28 March 2008 and then begins to decrease. Figure 2b also shows solar wind dynamic pressure which also shows a sudden increase on 26 March 2008. The AE index (Figure 2b) also shows an increase on 26 March 2008 and remains high up to 28 March and then begins decreasing. All these parameters indicate the triggering of a geomagnetic disturbance during this period.

[14] The electrojet strength for this period has been examined to identify possible prompt penetration effects. The temporal variation of electrojet strength for the period of 24–27 March 2008 is illustrated in Figure 3. The inhibition of electrojet strength on the morning of 25 March 2008 seems to be coincident with the recovery phase of the minor disturbance and probably indicates the disturbance dynamo related westward electric field modulating the EEJ. A similar effect is also seen on the morning of 26 March. A dramatic increase in the electrojet strength is revealed on 26 March around noon close to the time of sudden commencement of the moderate disturbance. The electrojet strength reaches very high values of around 100 nT (for this low solar activity period). This is probably the signature of a prompt penetration electric field at the magnetic equator. Up until 31 March 2008, we can see evidence of the effects of disturbance dynamo and prompt penetration electric fields alternately in the morning and noon sectors, respectively.

3.2. Response of EIA Region to the Disturbances on 26 March 2008 Based on Tomographic Images, Magnetic Field Data, and Ionograms

[15] The time variations of electrojet strength for 24 and 26 March 2008 are shown in Figure 4. It is clearly seen that the EEJ on 26 March was comparable to that on 24 March in the period prior to 10:00 LT, while it is significantly enhanced thereafter. Close to noon on 26 March, there is a strong IMF B_z southward turning which results in very strong eastward electric field penetration. This is manifested as the intensification in the electrojet strength, postnoon on 26 March. The times for which tomograms are available are

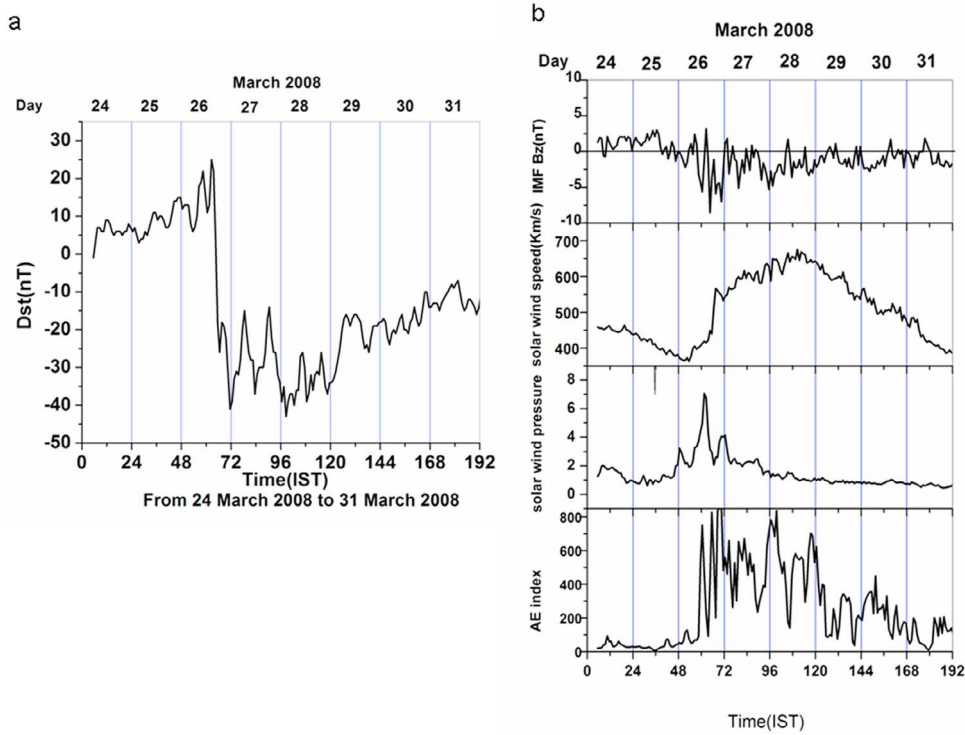


Figure 2. (a) Temporal variation of Dst for the period of 24–27 March 2008. (b) Temporal variation of IMF B_z , solar wind speed, solar wind dynamic pressure, and AE index the period of 24–31 March 2008.

marked in the Figure 3 (black curve for control day satellite pass (14:00 LT) and red lines for 26 March (11:45 and 14:40 LT) and 27 March (11:15 and 13:50 LT) satellite passes). As is evident from Figure 4 for 26 March, both the passes are for times when the electrojet strength is much intensified indicating the enhancement of the zonal electric field, whereas for 24 March the passes are for much lower electrojet strength and hence lower zonal electric field.

Therefore, an intense development of the anomaly is expected on 26 March for both the passes while for 24 March the EIA is expected to be much weaker. This inference is corroborated by the tomograms shown in Figures 5 (middle) and 5 (bottom) for 26 March and Figure 5 (top) for 24 March. On 26 March the tomogram at 11:45 LT shows the anomaly development with the crest at $\sim 15^\circ$ geomagnetic

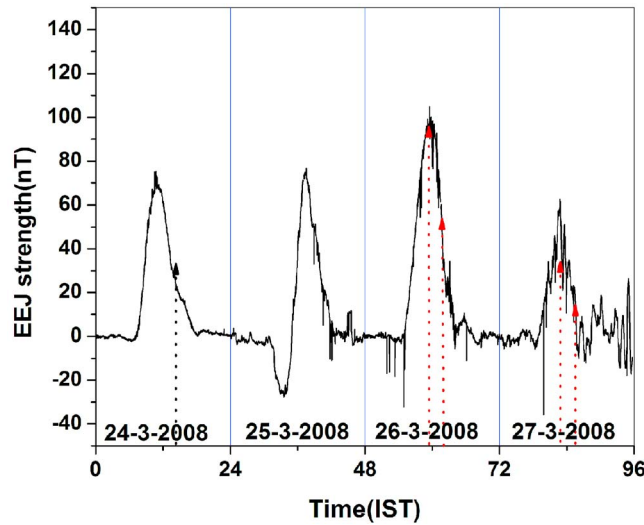


Figure 3. Temporal variation of electrojet strength for the period of 24–27 March 2008.

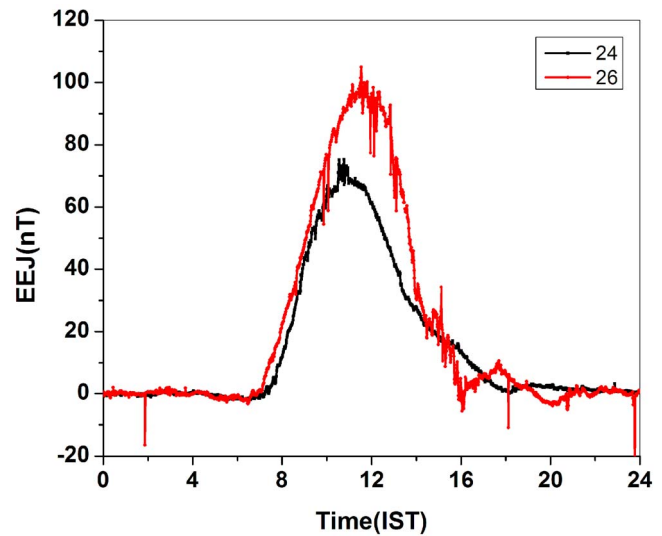


Figure 4. Temporal variation of electrojet strength for 24 and 26 March 2008.

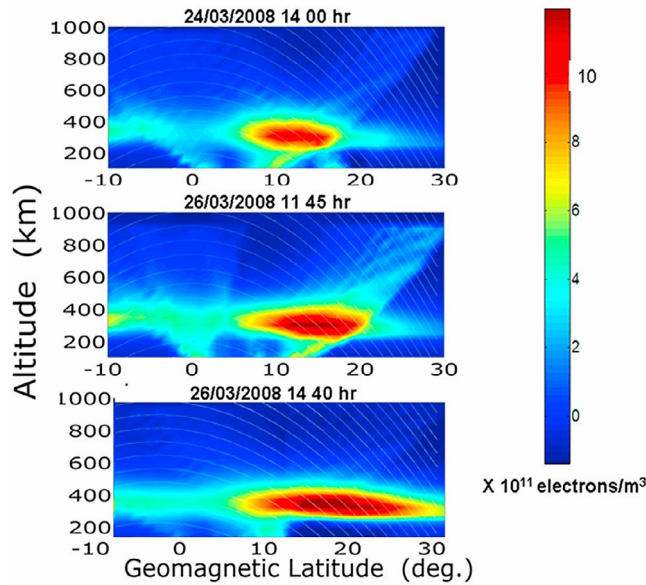


Figure 5. Tomograms showing the development of the EIA on 24 and 26 March 2008.

latitude. The next tomogram at 14:40 LT shows the crest at $\sim 20^\circ$ geomagnetic latitude, indicating an enhanced anomaly. In comparison to these tomograms, on 24 March at 14:00 LT (when the magnetic field was weaker), the intensity of the crest is also found to be much weaker and the location of the crest is $\sim 10^\circ$ geomagnetic latitude. Thus, on 26 March the two tomograms clearly bring out the spatio-temporal evolution of the EIA during this disturbed day. Further, Delhi (geomagnetic 20.67°N , 78°E) f_oF_2 values have also been examined (Figure 6) to confirm the enhancement of the EIA on 26 March in relation to 24 March. Data availability is limited during this period, and the available data points have been used for Figure 6. The f_oF_2 values at Delhi are significantly higher on 26 March compared to

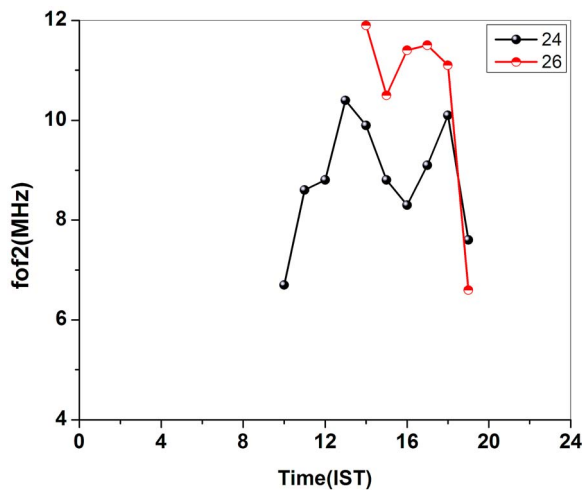


Figure 6. Time variation of f_oF_2 at Delhi on 24 and 26 March 2008.

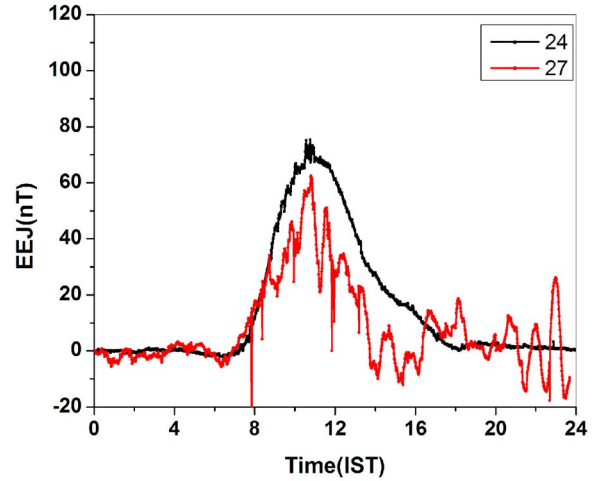


Figure 7. Temporal variation of electrojet strength for 24 and 27 March 2008.

24 March in the postnoon period indicating the latitudinal expansion of the EIA. The f_oF_2 values are not available at magnetic equatorial location of Trivandrum for 26 March.

3.3. Response of EIA Region to the Disturbances on 27 March 2008 Based on Tomographic Images, Magnetic Field Data, and Ionograms

[16] Time variation of electrojet strength on 24 and 27 March 2008 are depicted in Figure 7. The main phase of the disturbance which commenced close to 12:00 LT on 26 March occurred during the postnoon–midnight period of the same day. Correspondingly large enhancement is observed in the *AE* indices also (see Figure 2b). The consequent Joule heating effect in the polar region sets up a disturbance circulation which in turn results in disturbance dynamo induced westward electric fields manifesting at the magnetic equatorial location of Trivandrum and thus modulating the equatorial electrojet electric field. It is this effect that is responsible for the reduced EEJ strength on 27 March in comparison to that on 24 March. The disturbance induced modulation of h_mF_2 and f_oF_2 at Trivandrum on 27 March in comparison to that on the control day of 24 March are manifested in Figures 9 (for h_mF_2) and 10 (for f_oF_2). It is evident from Figure 9 that there is a significant inhibition in the vertical drift of the *F* layer in the prenoon phase of 27 March in comparison to the much larger vertical excursion of the layer on 24 March. The disturbance dynamo electric field on 27 March reduces the ionospheric zonal electric field and thereby the vertical drift of the *F* layer. As a consequence of this reduced vertical drift, there is a weakening of the fountain effect, which in turn results in higher f_oF_2 values (Figure 10) and reduced noon time bite out effect at Trivandrum on 27 March. The tomogram at 11:15 LT shows the presence of northern crest $\sim 9^\circ$ geomagnetic which is much less intense than on the control day (Figure 8, middle). The tomogram at 13:50 LT (Figure 8, bottom) on 27 March corresponds to a time when the electrojet strength is still weaker than at 11:15 LT. The intensity of the northern crest weakens in

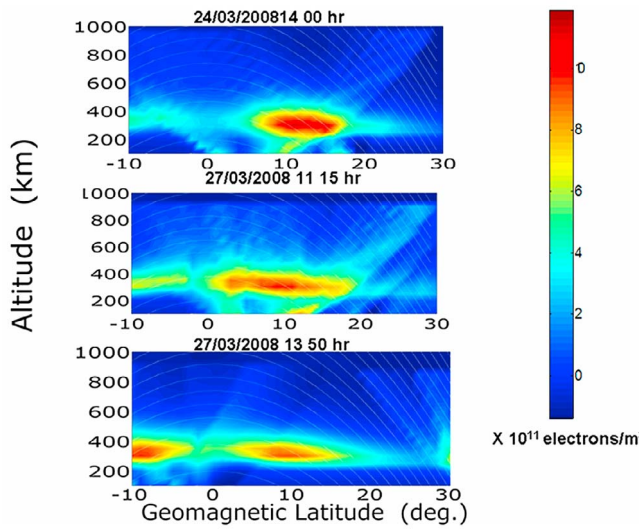


Figure 8. Tomograms showing the development of the EIA on 24 and 27 March 2008.

response to this reduced electrojet strength and the equatorward shift of the southern crest is visible.

3.4. First Time Observations of Large Enhancements in PEC in the EIA Region Over India During a Moderate Disturbance

[17] The latitudinal variation of PEC in the Indian EIA region has been examined for 24, 26, and 27 March using GPS and CRABEX TEC when simultaneous data are available from both the systems. Figures 11a, 11b, and 11c show the GPS, CRABEX and PEC variations on at 14:00 LT on 24 March, 11:45 LT on 26 March and 14:40 LT on 26 March, respectively. Similarly, Figures 11d, 11e, and 11f show the corresponding percentage PEC variations. On 24 March both GPS and CRABEX systems show the presence of a crest at

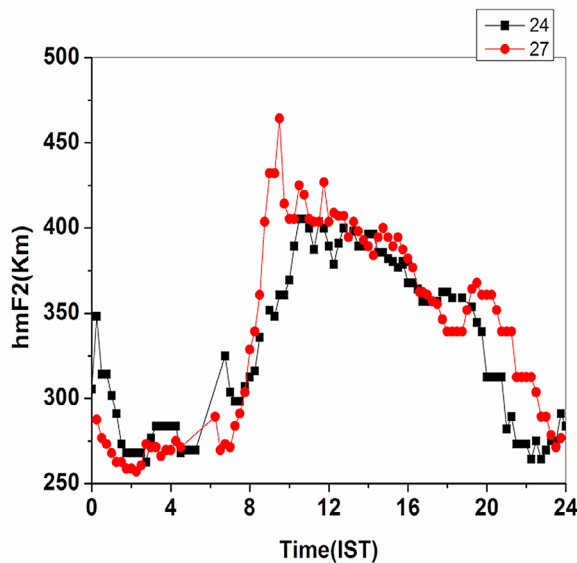


Figure 9. Time variation of $h_m F_2$ at Trivandrum on 24 and 27 March 2008.

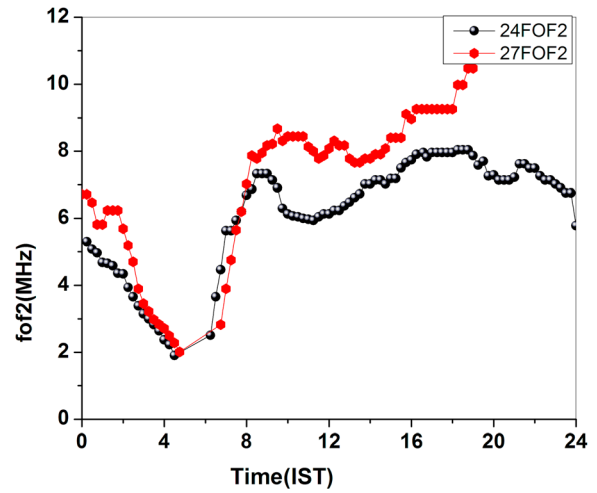


Figure 10. Time variation of $f_o F_2$ at Trivandrum on 24 and 27 March 2008.

15° geomagnetic latitude. The PEC on 24 March shows an increasing trend up to 20° geomagnetic latitude. The percentage PEC varies from ~30% at Bangalore to 60% at Delhi on this day. The increase in PEC during magnetically quiet period with latitude in the EIA region over India has been shown previously by Manju *et al.* [2008]. They presented the PEC variations from Trivandrum up to the latitude of Bangalore (8° geomagnetic latitude). Their percentage PEC variations of ~25% compare well with the present values obtained at Bangalore on 24 March. At 11:45 LT on 26 March, CRABEX data were unavailable at Delhi. The presence of the TEC crest is indicated at 15° geomagnetic latitude from GPS and CRABEX systems. But there seems to be significant depletion of PEC at the crest region and an increase at Bangalore in comparison to 24 March. This is in contrast to the increase in PEC with latitude observed during quiet times. The percentage contribution varies from 40% at Bangalore to 25% at Bhopal. At 14:40 LT, GPS and CRABEX TECs show the presence of a crest at the location of Bhopal (15° geomagnetic).

[18] Figures 12a, 12b, and 12c show the GPS, CRABEX, and PEC variations at 14:00 LT on 24 March, 11:15 LT on 27 March, and 13:50 LT on 27 March, respectively. Similarly, Figures 12d, 12e, and 12f show the corresponding percentage PEC variations. The PEC variations on the control day of 24 March are discussed above. At 11:15 LT on 27 March, CRABEX data show a crest at almost 10° geomagnetic latitude, while GPS data show an inhibited anomaly pattern. There seems to be a significant depletion of PEC at the crest region of Bhopal and an increase at Bangalore in comparison to 24 March. This is in contrast to the increase in PEC with latitude observed during quiet times. The percentage contribution varies from 30% at Bangalore to 45% at Delhi with minimum at Bhopal (20%). At 13:50 LT, CRABEX TEC shows the presence of crest at 10° (geomagnetic) while GPS still shows an inhibited anomaly. Correspondingly, the PEC shows spatial fluctuations with values of 32% at Bangalore, 20% at Bhopal, and 28% at Delhi. The PEC content itself shows a sharp decrease compared to 26 March 2008.

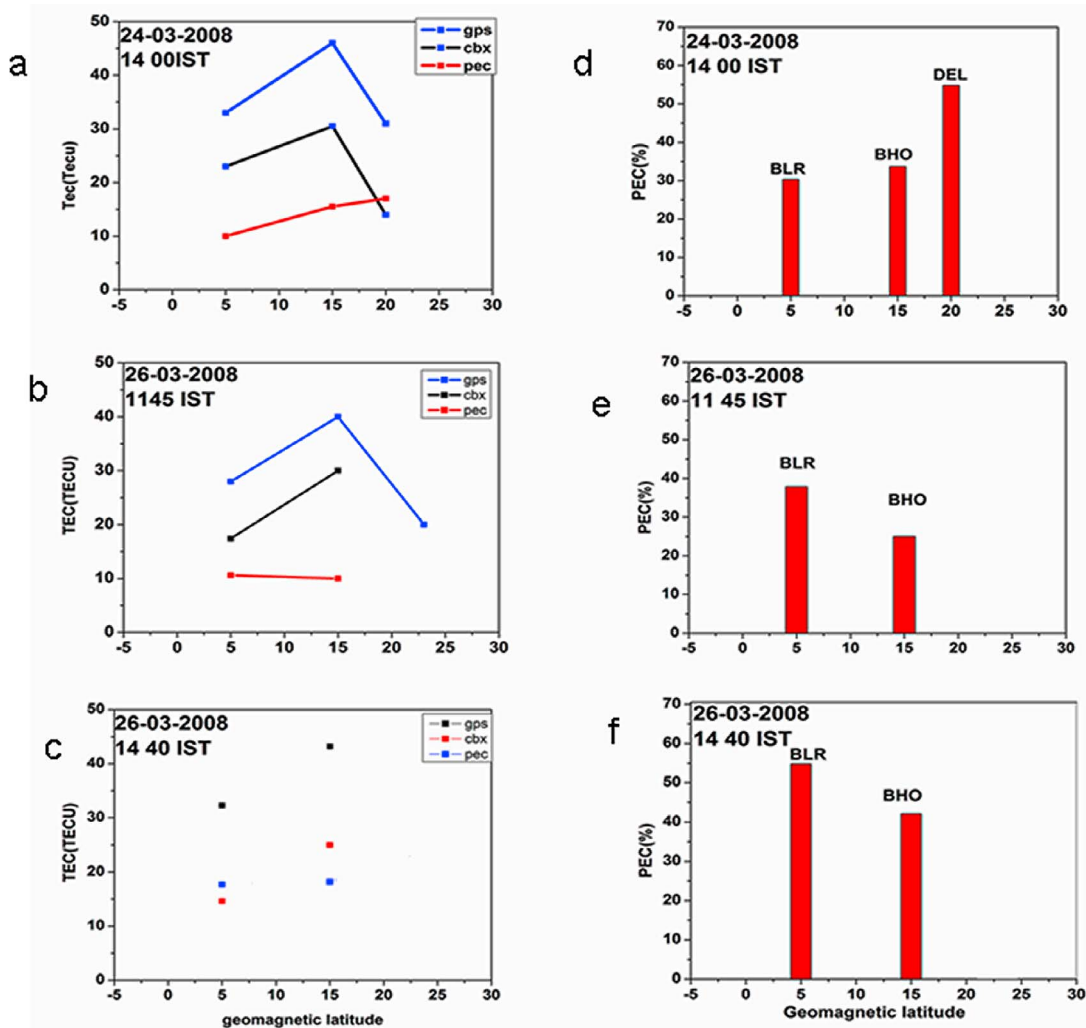


Figure 11. Percentage variation of PEC on 24 and 26 March 2008.

[19] The PEC variations observed on 26 and 27 March for the first time depict large spatial fluctuations in the EIA region over India for this moderate geomagnetic disturbance. Previously, such disturbance time spatial fluctuations have been reported only for very intense geomagnetic storms as reported by *Manju et al.* [2008].

4. Discussion

[20] It has been found that during geomagnetic disturbances, the equatorial ionospheric electric field gets enhanced due to penetration of another field of magnetospheric origin thereby resulting in latitudinal expansion as well as intensification of EIA [*Abdu et al.*, 1995; *Sastri et al.*, 2003; *Tsurutani et al.*, 2004; *Sobral et al.*, 1997]. In addition to this, the EIA is also modulated soon after event onset by intense disturbance-related electric fields originating from the magnetosphere-ionosphere interaction [*Blanc and Richmond*, 1980; *Fejer and Scherliess*, 1997]. Similarly, the large modulations of PEC during intense geomagnetic disturbances have also been reported [*Manju et al.*, 2008]. These studies underline the importance of ionospheric and

plasmaspheric variabilities during major geomagnetic storm events in view of the hazardous implications for GPS-based systems. The uniqueness of the present work is that substantial modulation of the equatorial and low-latitude ionosphere-plasmasphere system is observed for the first time even for a moderate geomagnetic disturbance. This disturbance had a sudden commencement around noon on 26 March 2008. The main phase ended around midnight of the same day. This was followed by a highly oscillatory recovery phase. The analysis reveals an enhanced EIA on 26 March after sudden storm commencement due to prompt penetration electric fields. On 27 March, during the recovery phase a disturbance dynamo-induced weakening of the EIA is clearly brought out by all the available data. On 27 March one interesting observation is the disturbance-induced spatial fluctuations in TEC brought out by the tomograms. One major highlight of the present result is that whenever simultaneous data sets are available, five station tomograms have been generated using absolute TEC data obtained from the Indian CRABEX network. These are the first five station tomograms in the world, encompassing the entire northern EIA region from the crest to the trough, and therefore it is a

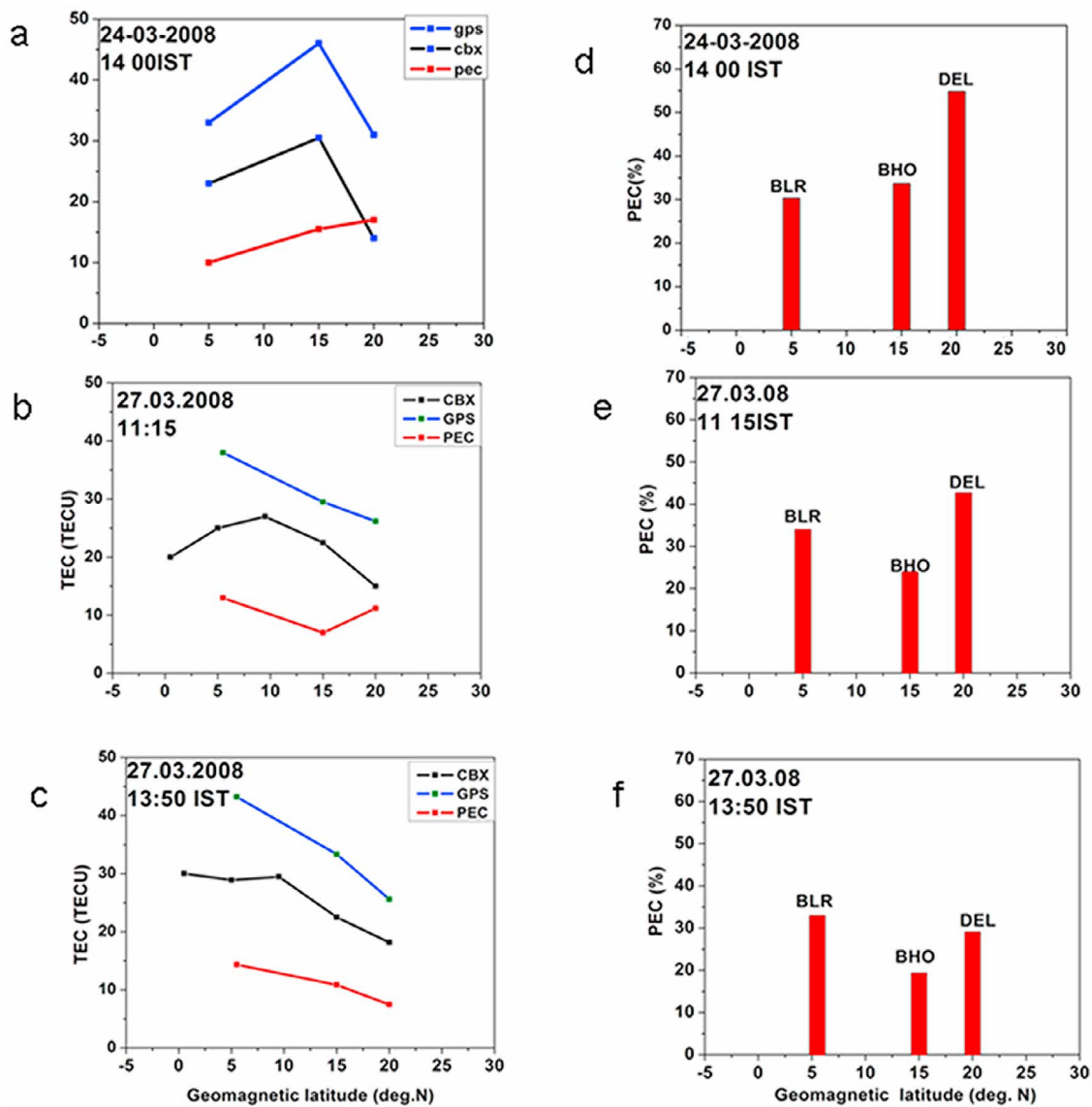


Figure 12. Percentage variation of PEC on 24 and 27 March 2008.

very momentous achievement for the Indian CRABEX program. The results obtained from the tomograms corroborate well with the concurrent observations made using other techniques as has been shown in section 3. Therefore, this study unambiguously demonstrates the efficacy of the tomographic technique in investigating storm-induced modulations of the EIA.

[21] Another important aspect that is brought out by this study is the significant spatial modulations of PEC in the EIA region during this moderate storm. The PEC values vary from 7 to 15 TECU during the storm period at different latitudes. Previously, such spatial fluctuations in PEC have been reported during intense storms, but it now seems that even moderate storms are susceptible to such PEC fluctuations. In the context of the increased use of GPS system for positioning and navigation purposes, measurement accuracies of better than 3 TECU are required. With single-frequency GPS users resorting to ionospheric models

without including PEC variations for removing ionospheric error, the derived position information will be highly erroneous at equatorial and low-latitude regions especially during magnetically disturbed periods. A complete understanding of the behavior of the upper atmosphere demands more investigations on the plasmasphere and factors that modulate the plasmaspheric electron content. Future modeling and experimental studies on the PEC variations need to be carried out to bring out the physics behind the spatial and temporal modulations of PEC.

5. Conclusions

[22] This paper for the first time reports large PEC contribution at equatorial and low-latitude regions over India during a moderate geomagnetic disturbance. It reiterates the need for more investigations into the plasmaspheric dynamics in view of the substantial modulations of PEC

occurring even during such moderate disturbances. This paper also presents, for the first time, five station tomograms encompassing the entire northern EIA region and unequivocally demonstrates the effectiveness of tomographic technique in investigating storm induced modulations of the EIA.

[23] **Acknowledgments.** This work was supported by Department of Space, Government of India. One of the authors, Lijo Jose, gratefully acknowledges the financial assistance provided by the Indian Space Research Organization through Research Fellowship. Authors thank ACE team (<http://omniweb.gsfc.nasa.gov/ow.html>) and WDC (Kyoto) for providing the geomagnetic data. The authors would also like to acknowledge Raj Dabas and his team, NPL, New Delhi for providing ionosonde data.

[24] Robert Lysak thanks James Whalen and another reviewer for their assistance in evaluating this paper.

References

- Abdu, M. A., I. S. Batista, G. O. Walker, J. H. A. Sobral, N. B. Trivedi, and E. R. de Paula (1995), Equatorial ionospheric fields during magnetospheric disturbances: Local time/longitudinal dependences from recent EITS campaigns, *J. Atmos. Sol. Terr. Phys.*, *57*, 1065–1083, doi:10.1016/0021-9169(94)00123-6.
- Appleton, E. V. (1946), Two anomalies in the ionosphere, *Nature*, *157*, 691–693, doi:10.1038/157691a0.
- Austen, J. R., S. J. Franke, and C. H. Liu (1988), Ionospheric imaging using computerized tomography, *Radio Sci.*, *23*(3), 299–307, doi:10.1029/RS023i003p00299.
- Blanc, M., and A. D. Richmond (1980), The ionospheric disturbance dynamo, *J. Geophys. Res.*, *85*, 1669–1686, doi:10.1029/JA085iA04p01669.
- Burrage, M. D., V. J. Abreu, N. Orsini, C. G. Fesen, and R. G. Roble (1992), Geomagnetic activity effects on the equatorial neutral thermosphere, *J. Geophys. Res.*, *97*, 4177–4187, doi:10.1029/91JA02439.
- Fejer, B. G., and J. T. Emmert (2003), Low latitude ionospheric disturbance electric field effects during the recovery phase of the 19–21 October 1998 magnetic storm, *J. Geophys. Res.*, *108*(A12), 1454, doi:10.1029/2003JA010190.
- Fejer, B. G., and L. Scherliess (1997), Empirical models of storm time equatorial zonal electric fields, *J. Geophys. Res.*, *102*, 24,047–24,056, doi:10.1029/97JA02164.
- Fuller-Rowell, T. J., M. V. Codrescu, B. G. Fejer, W. Borer, F. Marcos, and D. N. Anderson (1997), Dynamics of the low latitude thermosphere: Quiet and disturbed conditions, *J. Atmos. Sol. Terr. Phys.*, *59*, 1533–1540, doi:10.1016/S1364-6826(96)00154-X.
- Leitinger, R. (1994), Data from orbiting navigation satellites for tomographic reconstruction, *Int. J. Imaging Syst. Technol.*, *5*, 86–96, doi:10.1002/ima.1850050205.
- Leitinger, R., G. Schmidt, and A. Tauriainen (1975), An evaluation method combining the differential Doppler measurements from two stations that enables the calculation of electron content of the ionosphere, *J. Geophys.*, *41*, 201–213.
- Lu, G., X. Pi, A. D. Richmond, and R. G. Roble (1998), Variations of the total electron content during geomagnetic disturbances: A model/observation comparison, *Geophys. Res. Lett.*, *25*, 253–256, doi:10.1029/97GL03778.
- Manju, G., S. Ravindran, C. V. Devasia, S. V. Thampi, and R. Sridharan (2008), Plasmaspheric electron content (PEC) over low latitude regions around the magnetic equator in the Indian sector during different geophysical conditions, *J. Atmos. Terr. Phys.*, *70*, 1066–1073, doi:10.1016/j.jastp.2008.01.006.
- Rama Rao, P. V. S., K. Niranjan, D. S. V. V. D. Prasad, S. Gopi Krishna, and G. Uma (2006), On the validity of the ionospheric pierce point (IPP) altitude of 350 km in the Indian equatorial and low-latitude sector, *Ann. Geophys.*, *24*, 2159–2168, doi:10.5194/angeo-24-2159-2006.
- Sastri, J. H., R. Sridharan, and T. K. Pant (2003), Equatorial ionosphere thermosphere system during geomagnetic storms, in *Disturbances in Geospace: The Storm-Substorm Relationship*, *Geophys. Monogr. Ser.*, vol. 142, edited by A. S. Sharma, Y. Kamide, and G. S. Lakhina, pp. 185–203, AGU, Washington, D. C.
- Sobral, J. H. A., M. A. Abdu, W. D. González, B. T. Tsurutani, I. S. Batista, and A. L. C. de González (1997), Effects of intense storms and substorms on the equatorial ionosphere/thermosphere system in the American sector from ground based and satellite data, *J. Geophys. Res.*, *102*(A7), 14,305–14,313, doi:10.1029/97JA00576.
- Sreeja, V., S. Ravindran, T. K. Pant, C. V. Devasia, and L. J. Paxton (2009), Equatorial and low-latitude ionosphere-thermosphere system response to the space weather event of August 2005, *J. Geophys. Res.*, *114*, A12307, doi:10.1029/2009JA014491.
- Sreelatha, P., S. Ravindran, and C. V. Devasia (2005), A method of time synchronization between the different ground receiver stations of the Coherent Radio Beacon Experiment using GPS, paper A07.2(01592) presented at General Assembly, URSL, New Delhi, India.
- Thampi, S. V., T. K. Pant, S. Ravindran, C. V. Devasia, and R. Sridharan (2004), Simulation studies on the tomographic reconstruction of the equatorial and low latitude ionosphere in the context of the Indian tomography experiment: CRABEX, *Ann. Geophys.*, *22*, 3445–3460, doi:10.5194/angeo-22-3445-2004.
- Thampi, S. V., et al. (2007), Coherent Radio Beacon Experiment (CRABEX) for tomographic imaging of the equatorial ionosphere in the Indian longitudes: Preliminary results, *Adv. Space Res.*, *40*, 436–441, doi:10.1016/j.asr.2007.01.054.
- Tsurutani, B., et al. (2004), Global dayside ionospheric uplift and enhancement associated with interplanetary electric fields, *J. Geophys. Res.*, *109*, A08302, doi:10.1029/2003JA010342.

S. Alex, Indian Institute of Geomagnetism, Navi Mumbai, 410218 India.
L. Jose, G. Manju, N. Mridula, T. K. Pant, and S. Ravindran, Space Physics Laboratory, Vikram Sarabhai Space Centre, Trivandrum, Kerala 695 022, India. (nmridu@gmail.com)